Hindawi
Journal of Nanomaterials
Volume 2023, Article ID 9916777, 17 pages
https://doi.org/10.1155/2023/9916777

Research Article

Silver Nanoparticles Biosynthesized Using *Azadirachta indica* Fruit and Leaf Extracts: Optimization, Characterization, and Anticancer Activity

Njud S. Alharbi[1] **and Nehad S. Alsubhi**[2]

[1]*Department of Biological Sciences, Faculty of Science, King Abdulaziz University, Jeddah 21589, Saudi Arabia*
[2]*Department of Biology, Collage of Science, University of Jeddah, Jeddah, Saudi Arabia*

Correspondence should be addressed to Nehad S. Alsubhi; 04102763@uj.edu.sa

Received 7 December 2022; Revised 6 August 2023; Accepted 12 October 2023; Published 26 October 2023

Academic Editor: Zhengwei Huang

Copyright © 2023 Njud S. Alharbi and Nehad S. Alsubhi. This is an open access article distributed under the Creative Commons Attribution License, which permits unrestricted use, distribution, and reproduction in any medium, provided the original work is properly cited.

Silver nanoparticles (AgNPs) are becoming increasingly important for various crucial applications, including antimicrobial, anticancer, catalytic, and anti-inflammatory. AgNPs biosynthesized from plant extracts have attracted considerable attention because of their eco-friendliness, simplicity, cost-effectiveness, and stability. This study investigated the potential of using fruit and leaf extracts of the medicinal plant *Azadirachta indica* as a capping and reducing agent for the biosynthesis of AgNPs. The size, shape, and optical properties of AgNPs significantly affect their chemical, physical, and biological activity. Therefore, this study optimized the biosynthesis conditions as a first attempt for *A. indica* fruit extracts to produce AgNPs with precise morphology. Subsequently, the biologically manufactured AgNPs were characterized using suitable techniques. Their potential anticancer activities were examined against in vitro human lung and breast cancer (H1975 and MCF-7) cell lines. The AgNPs were stable, with a high yield and a spherical shape, ranging in size from 14 to 19 nm and exhibiting an absorption band between 420 and 440 nm. The AgNPs biosynthesized using *A. indica* fruit and leaf extracts were shown to be highly toxic against in vitro H1975, with IC_{50} of 62.2 and 91 μg/mL, respectively. The IC_{50} values were 67.5 and 68.7 μg/mL when testing against the MCF-7 cells. These findings suggest that plant-derived nanoparticles have enormous potential for future biomedical applications, which warrants further investigation.

1. Introduction

Nanotechnology plays a crucial role in science and requires the manipulation of matter to give rise to new structures, devices, and materials. Notably, the manipulation of matter occurs at a near-atomic scale, which stipulates the number of particles required. Nanotechnology was first introduced in 1959 by Richard Feynman, a Nobel Prize winner, and gained considerable attention, leading to its development in 1974.

Nanoparticles (NPs) are small molecules ranging between 1 and 100 nm. Their different physical and chemical forms are not visible to the naked eye [1]. Based on the presence of a carbon atom, nanoparticles can be classified into two groups: organic and inorganic. Inorganic nanoparticles include metallic NPs, such as gold and silver, and semiconductor NPs, such as zinc oxide, titanium, and magnetic nanoparticles. Recently, inorganic nanoparticles have been widely used in many applications owing to their promising properties. For example, these metallic particles have been studied as medical agents for treating various diseases [2]. Currently, the most common types of nanoparticles are semiconductors, metals, carbon-based, ceramic, polymeric, and lipid-based nanoparticles.

In recent studies, silver nanoparticles (AgNPs) are the most popular metal nanoparticles [3]. AgNPs have gained immense importance, primarily because of their large surface area, which enables coordination with many ligands, a feature not commonly found in many other types of nanoparticles [4]. The chemical, biological, and physical properties of AgNPs make them good candidates for various applications in pharmaceuticals, water treatment, biolabeling, food

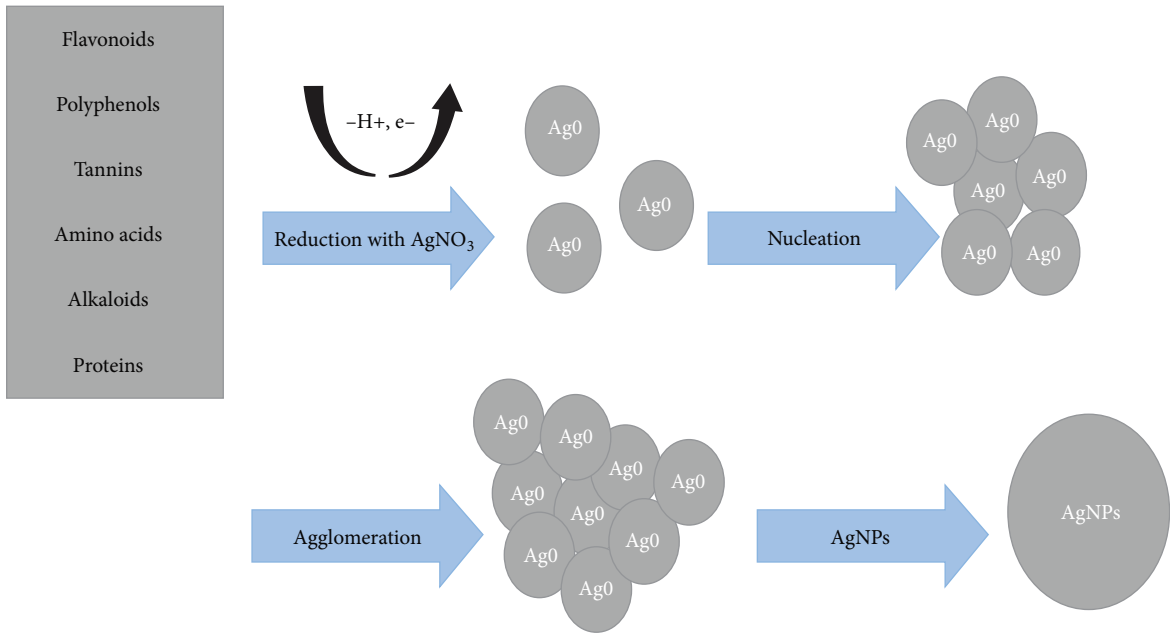

Figure 1: Mechanisms of biosynthesis AgNPs using plants.

industries, optics, textile coatings, catalysis, light emitters, energy science, integrated circuits, antimicrobial deodorant fibers, sensors, and drug delivery [5]. AgNPs have different shapes, including octagonal, diamond, and thin sheets, but a spherical shape is preferable in most applications [6]. AgNPs can be formulated chemically, physically, or biologically [7]. Chemical methods may result in AgNPs retaining toxins during the synthesis [8]. Physical methods may require high pressure and irradiation [9]. Biological methods that employ bacteria, fungi, and yeast to synthesize AgNPs ranging from 1 to 100 nm might be an alternative and are considered safe for humans and the environment [10]. Green or biological nanotechnology can improve the quality of life in several fields, including food, biomedical, and agricultural [11]. In addition, the nanoscale provides higher surface-to-volume ratios, which allow them to be applied in a wide range of fields, including antibacterial properties, medicine, diagnostics, anticorrosion, microelectronics, catalysis, biofertilizers, and nanosensors [12]. In addition, large-scale nanoparticles can be synthesized with green chemical processes, which can also be used to decrease pollution by absorbing environmental toxins and acting as a green corrosion inhibitor in acidic and basic media. It is also helpful for therapeutic applications, corrosion research, and cytotoxicity research [13]. The synthesis process mainly requires metal precursors ($AgNO_3$), reducing agents, stabilizing agents, and capping agents [14].

The use of medicinal plants to manufacture AgNPs has been previously studied [15–17]. Extracts from medicinal plants are economical, energy efficient, and environmentally friendly [18]. Using green chemistry to synthesize nanoparticles gave a hint for molecules consisting of biologically active plant extracts, which could reduce and stabilize the process [12]. The synthesis of AgNPs from plants is a simple two-step process. The first step involves the reduction of silver ions (Ag^+) to Ag. The second step is stabilization and agglomeration, leading to AgNPs forming (Figure 1) [5]. The hydroxyl groups involved in phytochemicals in plants, including flavonoids, enzymes, tannins, alkaloids, amino acids, and proteins, are mainly responsible for stabilizing and reducing Ag^+ to Ag^0 [8]. Reducing the Ag^0 further results in growing silver nuclei, hence forming AgNPs.

Biosynthesizing AgNPs from plant extracts is relatively easy, simple, and inexpensive (Figure 2). However, plant extract-based AgNP synthesis has a few limitations that must be addressed. For instance, phytochemicals may change during plant growth owing to internal/environmental exposure, affecting the reproducibility, homogeneity, and polydispersity of AgNPs. AgNPs may aggregate when synthesized with plant extracts, resulting in a large surface area. Furthermore, the diversity and complexity of plant extracts used in photochemical synthesis pose a significant challenge in understating their roles in regulating the shape and size of AgNPs under experimental conditions.

Azadirachta indica is a widely used medicinal plant in South and Southeast Asia and is grown in many parts of the world owing to its health benefits [19]. The extracts have been shown to cure various ailments and are used as fertilizers [20]. The biosynthesis of AgNPs employing leaf extract from *A. indica* has been reported in various studies [21, 22]. *A. indica* extract is vital for synthesizing AgNPs because of its flavanones and terpenoids, which stabilize AgNPs [22].

Cancer is a genetic disease caused by the mutation, amplification, or abnormal expression of essential genes involved in cell fate regulation [23]. Globally, breast cancer is the most common form of cancer, followed by lung cancer, as reported by the World Health Organization in 2020. Despite the significant investment of 5.5 billion dollars in breast cancer research over the past 20 years [24], the underlying causes of this disease are still unknown. Current

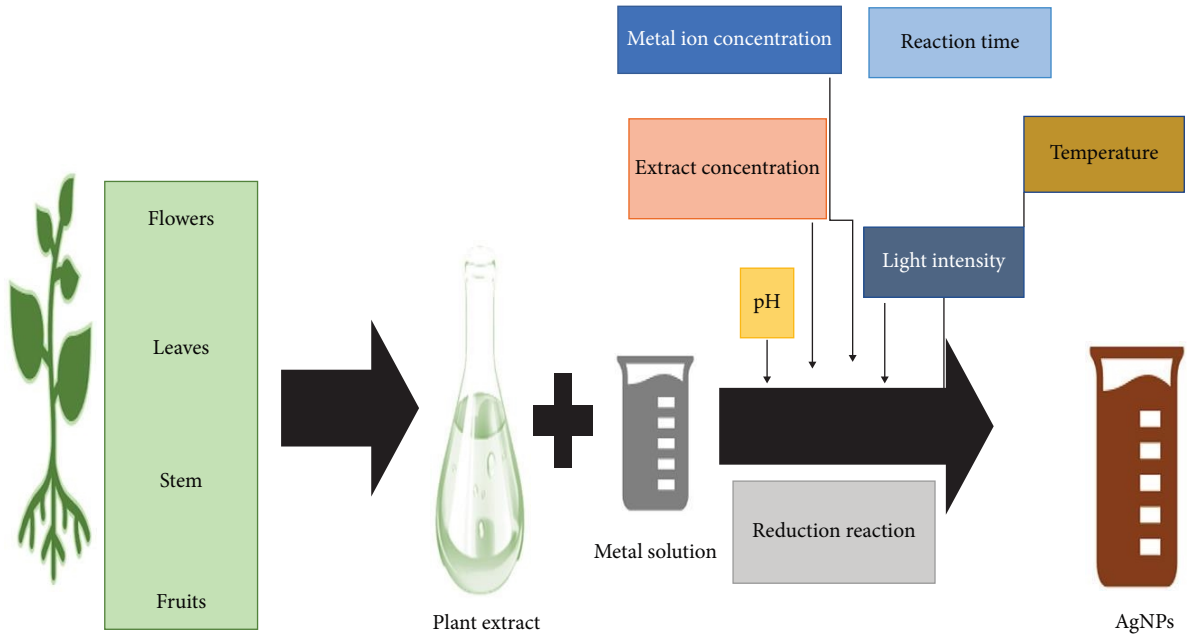

Figure 2: Plant-mediated synthesis of AgNPs.

medicines often prove fatal to patients because of their undesirable side effects. Thus, developing alternative tumor medicines with fewer side effects is necessary. In addition to other research areas, the natural manufacturing of products from medicinal herbs is the most successful. Nanotechnology applications in biological systems have recently been designated as a novel category in translational and reformative therapies. AgNPs have recently attracted considerable interest because of their ability to damage DNA, destroy tumor cells, generate reactive oxygen species (ROS), and regulate signaling pathways [25]. In our previous study, we synthesized AgNPs from *A. indica* fruit extracts, which exhibited a decrease in A549 cell viability [25]. This is the first study to optimize the biosynthesis of AgNPs using *A. indica* fruit extracts or assess their anticancer effects in lung and/or breast cancer (H1975 and/or MCF-7) cells. Therefore, this study aimed to biosynthesize AgNPs using *A. indica* fruit and leaf extracts and optimize the synthesis conditions to form AgNPs with precise morphologies. In addition, the study also examined the toxicity of the biosynthesized AgNPs against in vitro H1975 and MCF-7 cells, achieving significant results.

2. Materials and Methods

2.1. Materials. Harvest and collection of *A. indica* leaves, and fruits took place in Makkah City, Saudi Arabia, on October 14th and March 13th, 2020, respectively. The breast cancer line, MCF-7, was obtained from King Fahd Medical Research Center at KAU, Jeddah, KSA. The nonsmall cell lung cancer cell line, H1975, was obtained from King Faisal Specialist Hospital & Research Center, Jeddah, KSA. In addition, the following reagents were purchased from Solarbio, China: fetal bovine serum (FBS), Dulbecco's modified Eagle medium (DMEM), phosphate-buffered saline (PBS), dimethyl sulfoxide (DMSO), 100 U/mL penicillin, 100 mg/mL streptomycin, and 3-(4,5-dimethylthiazol-2-yl)-2,5-diphenyltetrazolium bromide (MTT) dye.

2.2. Plant Preparation. As previously described [26], the fruits and leaves of *A. indica* were washed twice with tap water, rinsed twice with distilled water, and dried in the shade at 25°C (room temperature). The leaves and fruits were then powdered, kept in a sealed container, and stored at −20°C until use [27]. The preparation time for *A. indica* fruits and leaves was nearly identical.

2.3. Aqueous Plant Extraction. Plant extraction was performed as previously described [26]. Fruits and leaves (5 g) were suspended in 100 mL of deionized water in a 250 mL flask. The solution was boiled for 10 min at 100°C and then filtered using a coffee filter first to separate the large particles. Subsequently, further filtering was performed using Whatman No. 1 filter paper to obtain a clear solution. The extracts were then poured into an Erlenmeyer flask (250 mL) and refrigerated until further use. The *A. indica* leaves, fruits, and extracts are shown in Figure 3.

2.4. Synthesis of AgNPs. As described previously, 90 mL of 1 mM $AgNO_3$ solution was added separately to 10 mL of fruit and leaf extracts [28]. The mixture was placed at room temperature (25°C) until the sample color changed, centrifuged for 15 min at 12,000 rpm, the supernatant was removed, and the pellet was washed with deionized water. The centrifugation was repeated twice or thrice to remove any substances absorbed from the AgNPs. Figure 4 shows a schematic illustrating the synthesis of AgNPs using plant extracts. Finally, the samples were freeze-dried for further characterization and application.

2.5. Optimizing the AgNPs Synthesis. This study evaluated the effects of synthesis parameters, including extract concentration,

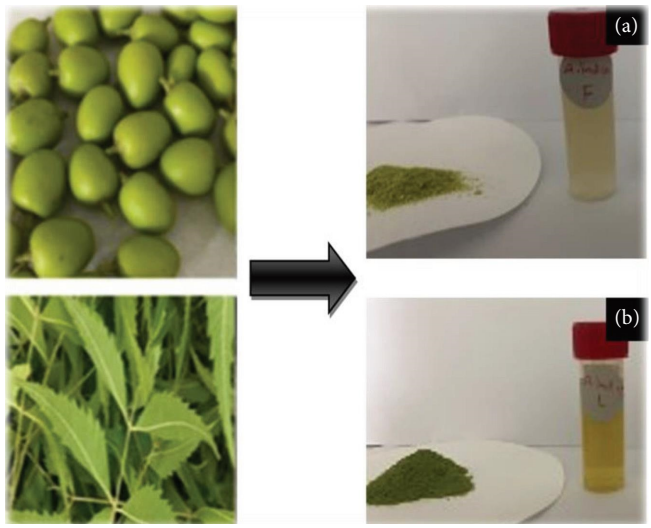

Figure 3: Plants and extracts. (a) *A. indica* fruit extract and (b) *A. indica* leaf extract.

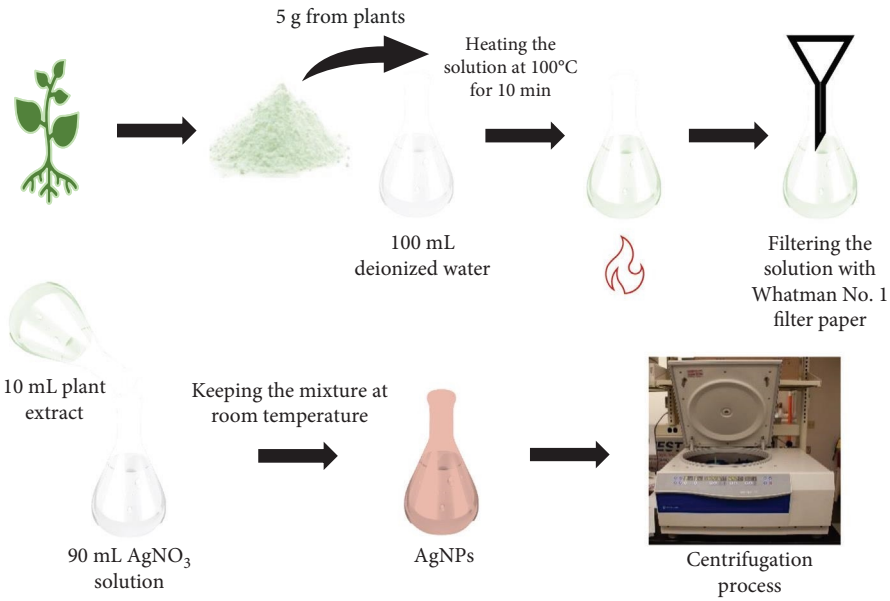

Figure 4: Schematic diagram of AgNPs synthesized using plant extracts.

temperature, pH, and light intensity, on the morphology and yield of AgNPs. The $AgNO_3$ solution (1 mM) remained constant despite all the conditions. The plant extracts and $AgNO_3$ solutions had a pH of 7. As previously described [29], AgNPs were synthesized using different extract concentrations: 10%, 20%, and 30% at a temperature of 25°C and a pH value of 7. As per a previous study [30], we synthesized AgNPs at various temperature values: 25, 40, 60, and 80°C using 10% extract concentration and pH 7. Moreover, acetic acid (CH_3COOH) and sodium hydroxide (NaOH) were added in small amounts to adjust various pH conditions (acidic at 4, neutral at 7, and basic at 9) that were employed to create AgNPs at 25°C and 10% extract concentration, as previously described [31]. The AgNPs were synthesized under different light conditions: dark, room light, and sunlight, using a 10% extract concentration at 25°C and pH 7, as previously described [32]. In addition, the $AgNO_3$ concentration and reaction time effect on the morphology of the AgNPs were extensively studied [21]. Although AgNPs can be synthesized using $AgNO_3$ concentrations ranging from 0.1 to 10 mM, 1 mM is the best $AgNO_3$ concentration for synthesizing AgNPs, as previously reported [33, 34]. Hence, this study used a 1 mM $AgNO_3$ concentration. Multiple reactions with different durations can increase the reduction rate and synthesize AgNPs with the appropriate morphology [35]. A previous study concluded that AgNPs were completely produced when plant extracts were incubated with $AgNO_3$ for 6 hr

[36]. Hence, increasing the reaction time increases the reduction rate of AgNP synthesis.

2.6. Characterization of AgNPs

2.6.1. Ultraviolet–Visible Spectroscopy. As previously described [26], 3 mL of AgNP solution was placed in a UV glass cuvette cell and analyzed using ultraviolet–visible (UV–Vis) spectroscopy at wavelengths ranging from 300 to 600 nm with a 1 nm resolution at room temperature (~25°C). Deionized water was used as a blank to calibrate the spectrophotometer.

2.6.2. Fourier Transform Infrared Spectroscopy. Fourier transform infrared (FTIR) spectroscopy (Thermo Fisher Scientific, Waltham, MA, USA) was used to examine the functional groups before and after the biosynthesis of AgNPs. Dried samples of plant extracts and AgNPs were analyzed by FTIR spectroscopy and scanned in the range of 600–4,000 cm^{-1} and at 4 cm^{-1} transmittances.

2.6.3. Field Emission Scanning Electron Microscopy. Field emission scanning electron microscopy (FESEM) was used to determine the shape and size of AgNPs. As previously described [37], a thin film of each biosynthesized AgNP sample was created by adding a few drops of the sample to a copper grid. The grid was allowed to dry at 25°C. The prepared samples were then examined using FESEM at magnifications of 250,000x and 120,000x (model Jeol 7600 F FESEM, Tokyo, Japan).

2.6.4. Dynamic Light Scattering and Zeta Potential. Dynamic light scattering (DLS) and zeta potential were used to measure the dynamic size distribution and surface charge of the synthesized AgNPs, respectively, using a Zetasizer (Malvern ZEN3600, Malvern Instruments, Malvern, UK). All nanoparticles were sonicated for 5 min before DLS and zeta potential analysis. As previously described [38], the AgNP solution was diluted with distilled water, and 1 mL of the sample was placed in a cuvette for analysis. The autocorrelation functions consist of an average of six runs of 10 s for each sample.

2.7. Anticancer Activity of AgNPs. The cytotoxicity of green-synthesized AgNPs against the cancer cell lines H1975 (lung cancer) and MCF-7 (breast cancer) was determined according to the methodology described in a previous study [39]. The cultivated cells were placed into 96-well microplates at 10,000 cells/well density for H1975 and 5,000 cells/well for MCF-7 in triplicate and incubated at 37°C with 5% CO_2. The cells were cultured in DMEM containing 10% FBS and 100 μg/mL penicillin/streptomycin. After reaching 70% confluence, the cells were exposed to variable concentrations of AgNPs ranging from 12.5 to 200 μg/mL, and 3% DMSO was used to dissolve powdered AgNPs. After 48 hr of incubation, the MTT assay was performed to determine the cytotoxicity of AgNPs by measuring absorbance at 570 nm using an enzyme-linked immunosorbent assay microplate reader. Cell cytotoxicity was determined by calculating the percentage of viable cells remaining using Equation (1):

$$\text{Cell viability } (\%) = \frac{\text{Absorbance of sample} - \text{Blank}}{\text{Absorbance of untreated cells} - \text{Blank}} \times 100. \quad (1)$$

3. Results and Discussion

3.1. Synthesis of AgNPs. As reported earlier, a change in the reaction solution (dark brown color) confirmed the formation of AgNPs. Surface plasmon resonance excitation and its bands, which result in the color change solution, are important for confirming the synthesis of AgNPs [40]. In addition, this indicates that the phytochemicals in the fruit and leaf extracts of *A. indica* magnificently reduced silver ions to Ag^0 in solution. *A. indica* fruit and leaf extracts were used to stabilize AgNPs, as the color of the solution remained unchanged after 6 months. In previous studies, the stabilization of nanoparticles has been achieved using chitosan oligosaccharide lactate or sebacic acid [41, 42]. Figure 5 shows the $AgNO_3$ and AgNP solutions before and after synthesis, with the color changing from bright green to a stable dark brown, indicating a complete reduction of Ag^+ into AgNPs [43].

3.2. Characterization of AgNPs

3.2.1. UV–Vis Spectroscopy Analysis. AgNPs exhibit a high surface plasmon resonance in an aqueous solution and emit light between 400 and 500 nm, depending on their size, shape, and morphology [44]. Thus, as shown in Figure 6, since no peak appears in the 400–500 nm range for extracts or $AgNO_3$, the peak wavelengths observed in this range should be only for nanoparticles. The absorption spectra of AgNPs were evaluated at different parameters (extract concentration, temperature, pH, and light intensity), illustrating the impact of these parameters on the morphology and yield of AgNPs.

(*1*) *Extract concentration*. To study the influence of extract concentrations, we biosynthesized AgNPs at different extract concentrations: 10%, 20%, and 30% at 25°C and pH 7. Figure 7 shows that the absorption intensity of AgNPs increases with increasing extract concentration. The results showed that fruits produced AgNPs with a higher absorption intensity than those formed by leaves, indicating that the fruits yield more nanoparticles than leaves. In addition, increasing the concentration of *A. indica* leaf extract from 10% to 30% shifted the absorbance (silver peak) from 434 to 410 nm, forming a smaller particle size. However, the particle size was stable when using *A. indica* fruit extract, as the silver peak appeared at a wavelength of 424 nm, regardless of the extract concentration. Furthermore, the color of the solution slowly changed to brown as the extract concentration increased, illustrating the slow reduction of Ag^+ to form Ag^0. These findings are consistent with previous studies [29, 45].

(*2*) *Temperature*. Figure 8 shows an increase in the growth of AgNPs with increasing temperature. For example, increasing the temperature from 25 to 80°C decreased the wavelength of the absorbance peak from 424 to 410 nm for

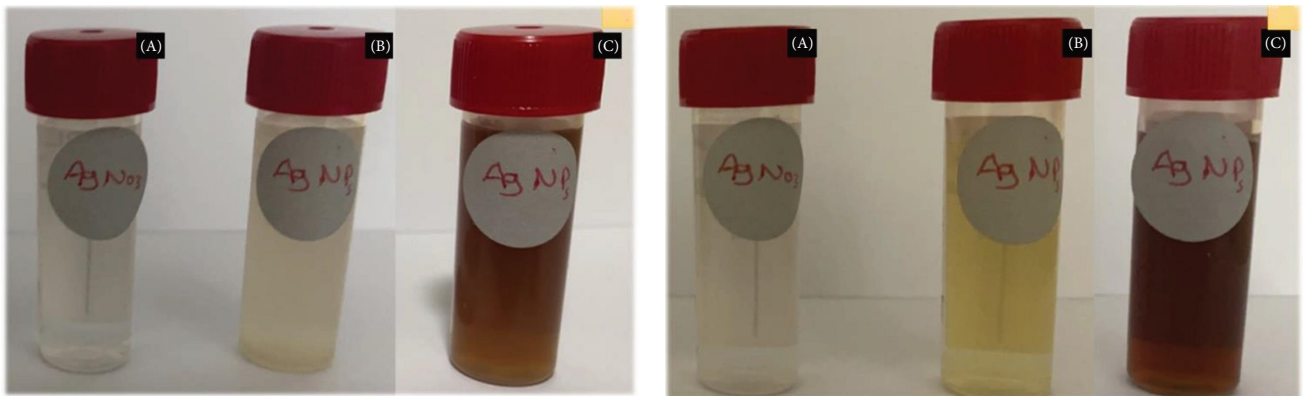

(a) (b)

Figure 5: (A) $AgNO_3$ solution, and (B and C) AgNPs solution before and after AgNP synthesis using (a) *A. indica* fruit extract and (b) *A. indica* leaf extract.

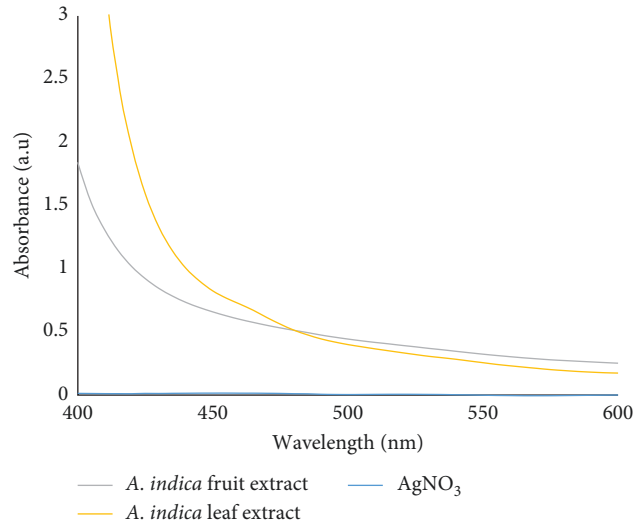

Figure 6: Absorption spectra of *A. indica* fruit and leaf extracts, and silver nitrate.

the AgNPs synthesized using *A. indica* fruit extracts, forming small-sized nanoparticles. Similar results were observed for AgNPs synthesized using *A. indica* leaf extract. Hence, high temperatures could promote nanoparticle growth because the higher kinetic energy of the particles at high temperatures enables faster bioreduction of silver ions. These findings are consistent with previously reported results [46, 47].

(*3*) *pH*. Different pH values (acidic at pH 4, neutral at pH 7, and basic at pH 9) were used to optimize the synthesis of AgNPs. Figure 9 shows that when the pH was increased to 9, higher absorption intensities were observed at 410 and 405 nm for AgNPs biosynthesized using *A. indica* fruits and leaves, respectively, illustrating the production of small nanoparticles. These findings confirm that pH can enhance the reduction rate of Ag^+, resulting in a brown color after a few seconds of adding silver nitrate solution to the extracts. High pH can improve the bioavailability of the functional groups in plant extracts, and similar results have been reported [46]. However, Verma and Mehata [46] reported that high pH resulted in the agglomeration and instability of nanoparticles in storage. At pH 7, absorbance peaks appeared at 425 and 429 nm for AgNPs synthesized from leaves and fruits, respectively. A previous study [47] demonstrated that pH 7 is the most suitable for synthesizing AgNPs compared to the other pH values. These findings suggest that a neutral environment can help form appropriately sized nanoparticles. The difference in absorbance between pH 7 and pH 9 may result from the fact that pH 7 reactions take 20 min to occur while pH 9 reactions take just a few seconds. By contrast, AgNPs were slowly synthesized at a pH value of 4. They had broad wavelengths with increasing peak absorption, thus forming large nanoparticles.

(*4*) *Light Intensity*. The AgNPs were synthesized under different light conditions (dark, room light, and sunlight), and the results are discussed in Figure 10. When exposed to sunlight, the absorbance intensity of the narrow peak increased, indicating the complete formation of AgNPs. A previous study using *A. indica* leaves reported that exposure to sunlight

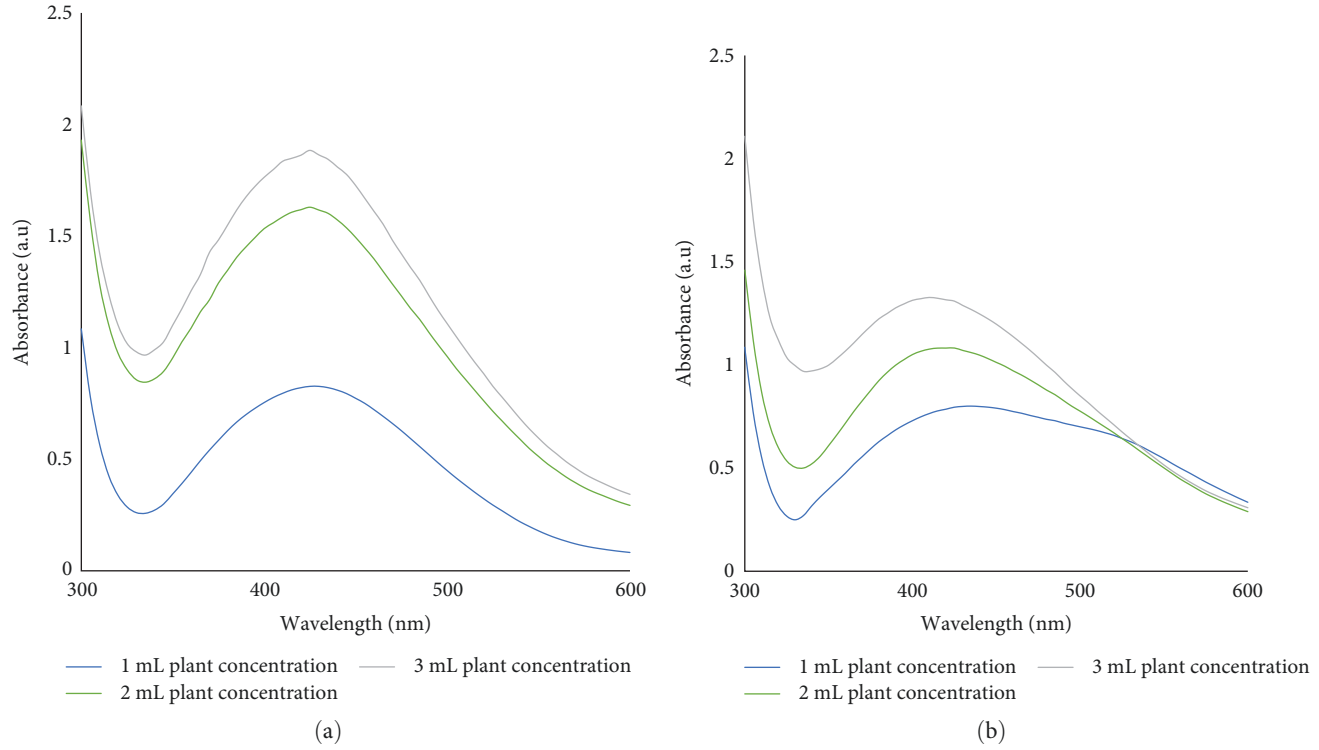

Figure 7: UV–Vis absorption spectra of AgNPs biosynthesized under different plant concentrations. (a) *A. indica* fruit extract and (b) *A. indica* leaf extract.

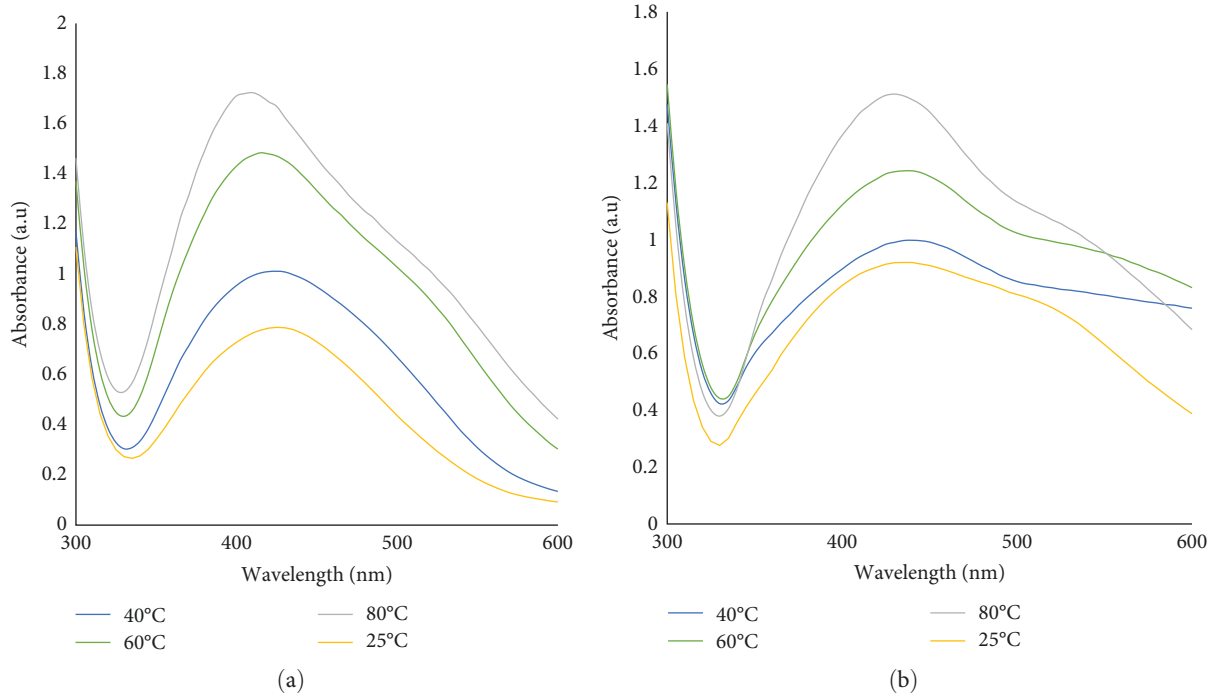

Figure 8: UV–Vis absorption spectra of AgNPs biosynthesized under different temperatures. (a) *A. indica* fruit extract and (b) *A. indica* leaf extract.

accelerated the formation of smaller AgNPs [48]. Owing to photon promotion, AgNPs are rapidly biosynthesized under sunlight. Furthermore, under both room light and sunlight conditions, the biosynthesized AgNPs had absorbance peaks at the same wavelengths, confirming that sunlight does not affect nanoparticle size but only catalyzes the reaction to obtain high yields of AgNPs. However, no nanoparticles were produced under dark conditions when leaf extract was

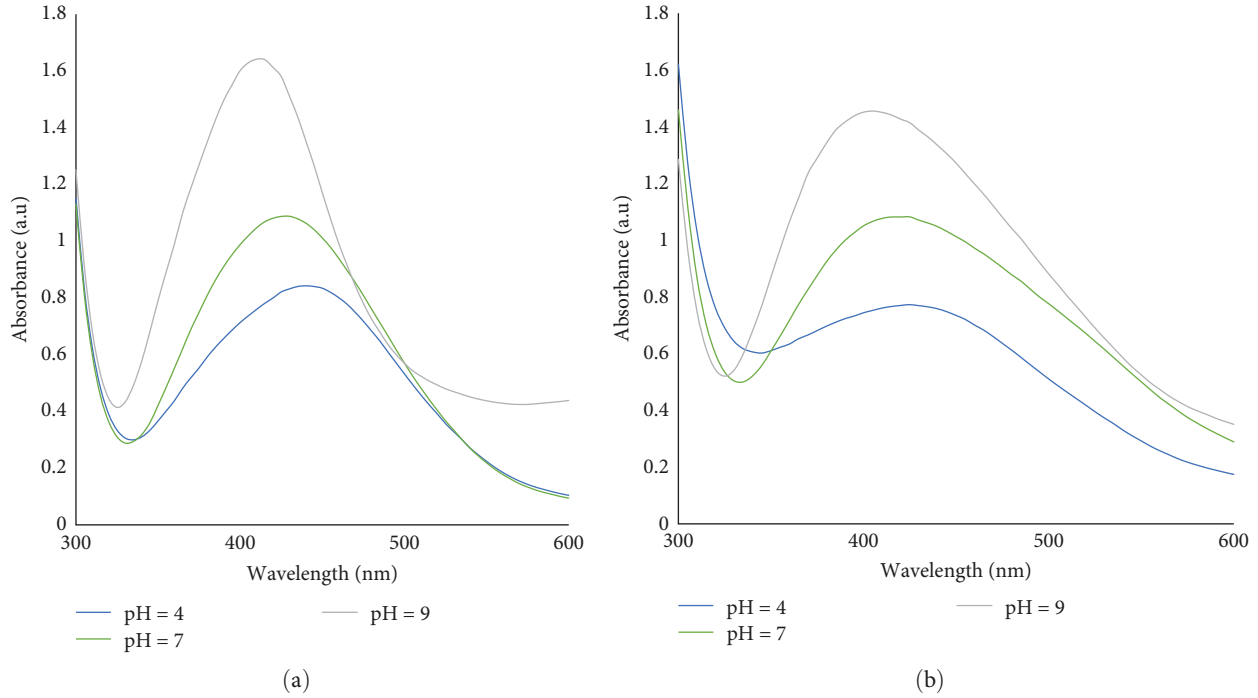

Figure 9: UV–Vis absorption spectra of AgNPs biosynthesized under different pH values. (a) *A. indica* fruit extract and (b) *A. indica* leaf extract.

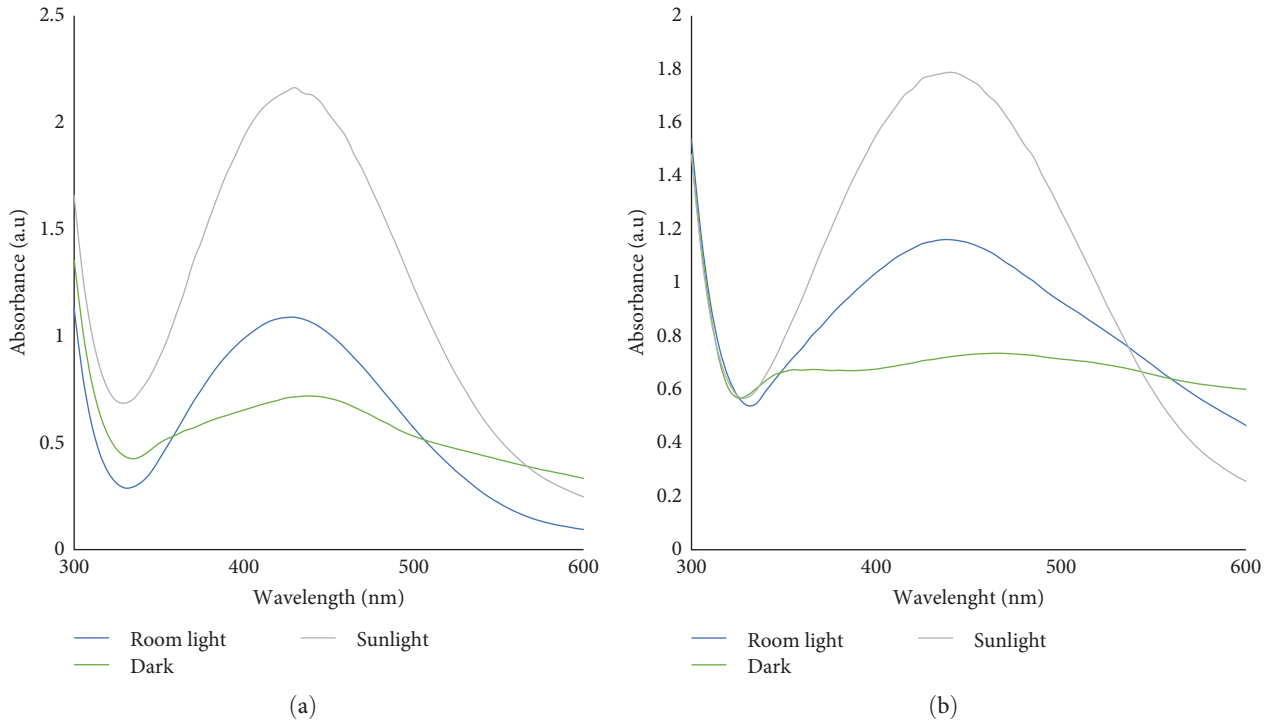

Figure 10: UV–Vis absorption spectra of AgNPs biosynthesized under different light intensities. (a) *A. indica* fruit extract and (b) *A. indica* leaf extract.

used. By contrast, the fruit extract could produce nanoparticles, which may be attributed to the difference in the phytochemicals in fruits and leaves. These results suggest that light plays a critical role in accelerating AgNP synthesis. A previous study reported that small AgNPs could be produced using pomelo peel extracts under direct sunlight [49].

The synthesis parameters (30% extract concentration, 80°C, pH 9, and room light) with the best results were

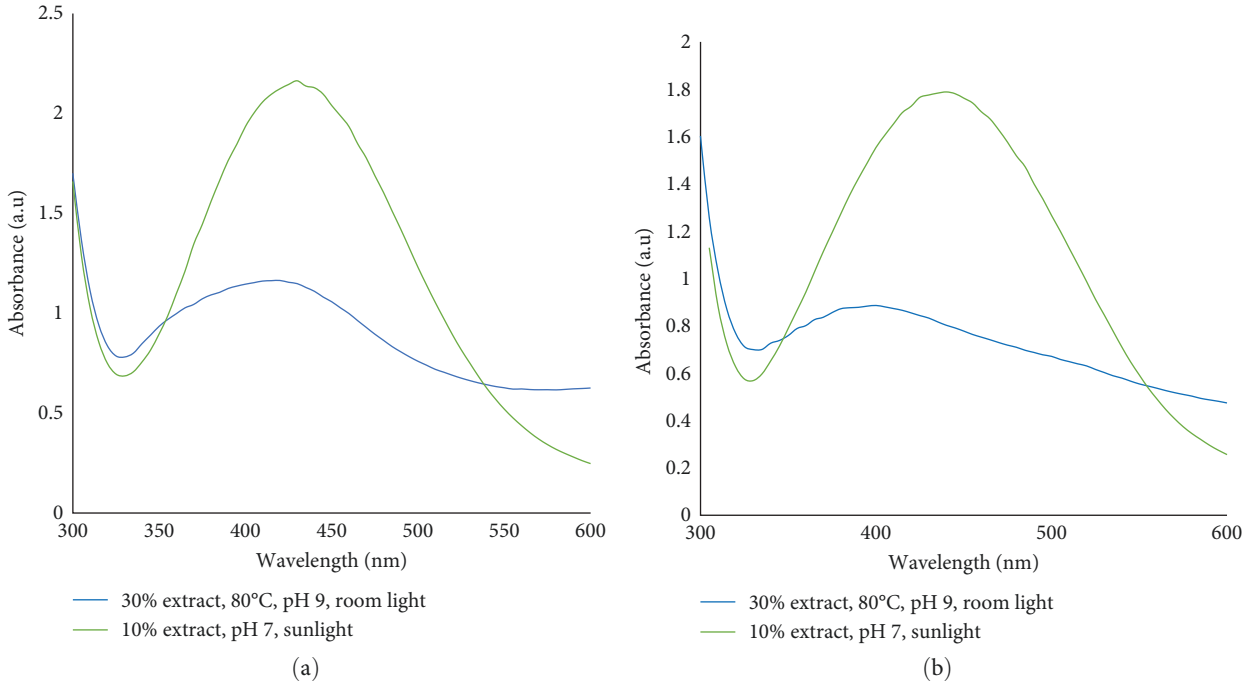

FIGURE 11: UV–Vis absorption spectra of AgNPs biosynthesized under (30% extract, 80°C, pH 9, room light) and (10% extract, pH 7, sunlight light) conditions. (a) *A. indica* fruit extract and (b) *A. indica* leaf extract.

used to synthesize the AgNPs, and the results are shown in Figure 11. Biosynthesized AgNPs with broad absorption peaks were observed, indicating particle aggregation. A previous study reported similar results [50]. The aggregation and growth of AgNPs accelerate at high temperatures upon adding plant extracts to the $AgNO_3$ solution, resulting in unstable AgNPs, which may lead to the degradation and loss of bioactive compounds [51]. Furthermore, AgNPs were synthesized at 10% extract concentration, pH 7, and sunlight, providing high yields and narrow peaks, as shown in Figure 11. These results optimized the synthesis parameters (10% extract concentration, pH 7, and sunlight light) for further investigations in this study.

3.2.2. FTIR Analysis. In the FTIR analysis, the AgNPs spectrum displayed several bands across the 600–4,000 cm^{-1} measurement range. Figure 12 shows the FTIR spectra of the biosynthesized AgNPs and the *A. indica* fruit and leaf extracts. The results show equal performance from both *A. indica* leaf and fruit extracts to bind and reduce Ag^+ through functional groups, owing to the similarity of the absorbance bands. The absorbance bands of the leaf extract were in the range of 3,300–3,340, 2,920–2,940, 1,600–1,630, 1,400–1,430, and 1,020–1,050 cm^{-1}. The bands around 3,300, 2,900, 1,600, 1,400, and 1,020 cm^{-1} correspond to the functional groups present in the sample. They also correspond to OH-bonding, confirming the existence of phenol, CH alkyl, C = N, NH, and CO stretching, respectively [52]. The band at 2,345 cm^{-1} was only observed in the fruit extract, corresponding to CH alkenes [53]. However, the peaks observed in both *A. indica* extracts disappeared in the AgNPs, suggesting that amino groups are partly utilized for stabilizing and encapsulating the nanoparticles. In addition, the band around 2,900 cm disappeared when synthesizing AgNPs from fruit extract, and it appeared when using leaf extract, suggesting that CH groups are also involved in nanoparticle synthesis. These findings agree with previously reported results [54] and [55]. *A. indica* extracts contain phenolics, flavonoids, and other bioactive compounds, which react to form AgNPs [56].

3.2.3. FESEM Analysis. Figures 13 and 14 show the spherical shapes with uniform distributions for both biosynthesized AgNPs. In addition, the average size of AgNPs synthesized from *A. indica* fruit and leaf extracts are 14.5 and 18.7 nm, respectively. An earlier study of *A. indica* leaf extract synthesized larger AgNPs with sizes of approximately 20–50 nm [21]. The FESEM images also showed a small aggregate of nanoparticles, possibly due to sample preparation for FESEM analysis, which agrees with this study [57]. The spherical nanoparticles interact better with cell surfaces, facilitating the uptake of these particles by cells and thus increasing their cytotoxicity [58]. Furthermore, AgNPs have size-dependent activity, with small-sized AgNPs more toxic to the cells [59].

3.2.4. DLS and Zeta Potential. DLS measurements revealed that AgNPs biosynthesized using *A. indica* fruit extract had a size of 245 nm, as shown in Figure 15(a). By contrast, a particle size of 160 nm was observed when using *A. indica* leaf extract, as shown in Figure 16(a). The particle sizes measured by DLS appear larger than those measured by FESEM because DLS includes bioorganic molecules encapsulating AgNPs [60]. Moreover, Van der Waals forces may increase the particle size of the solution. Furthermore, the results showed that AgNPs biosynthesized using *A. indica* fruit and leaf extracts

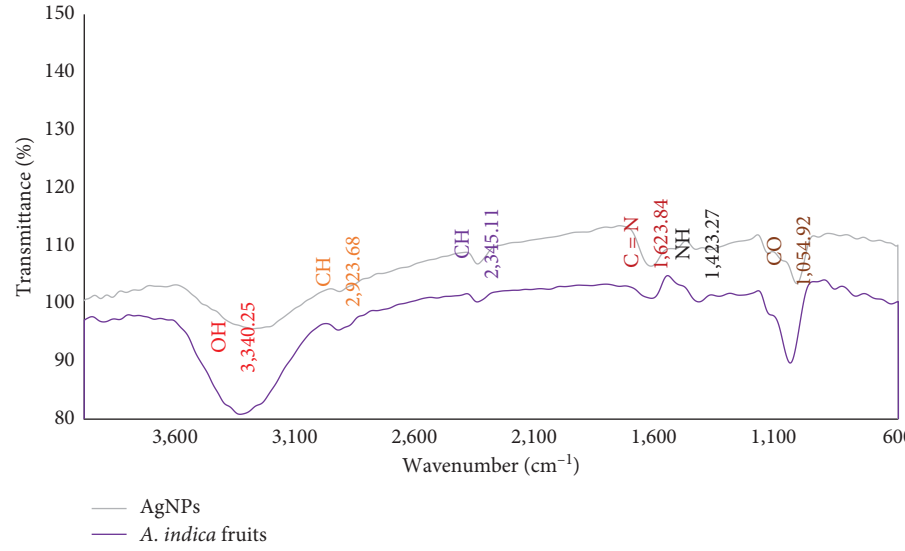

(a)

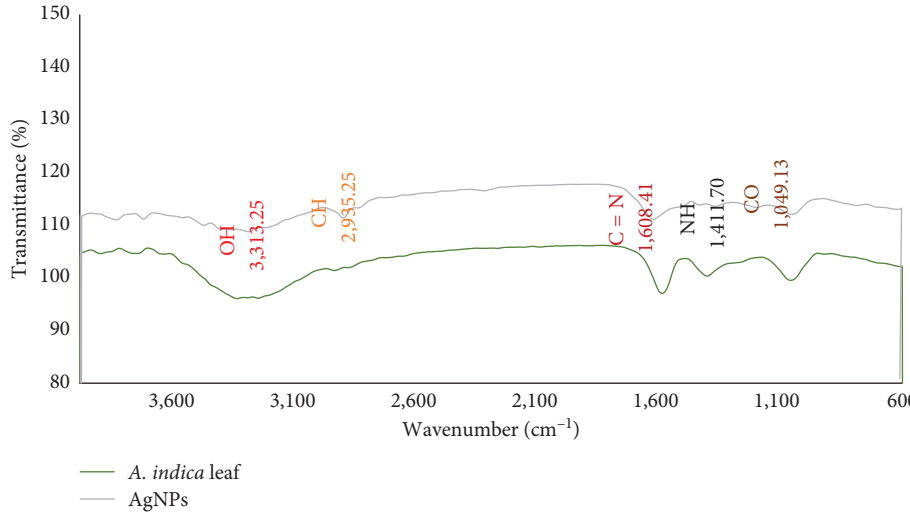

(b)

Figure 12: FTIR analysis of plant extract and biosynthesized AgNPs. (a) *A. indica* fruit extract and (b) *A. indica* leaf extract.

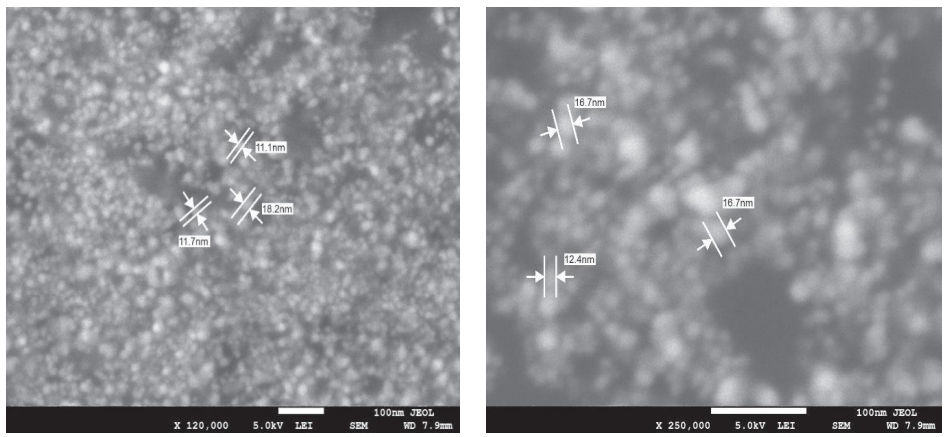

(a) (b)

Figure 13: FESEM image of AgNPs biosynthesized using *A. indica* fruit extract at magnification. (a) 120,000x and (b) 250,000x.

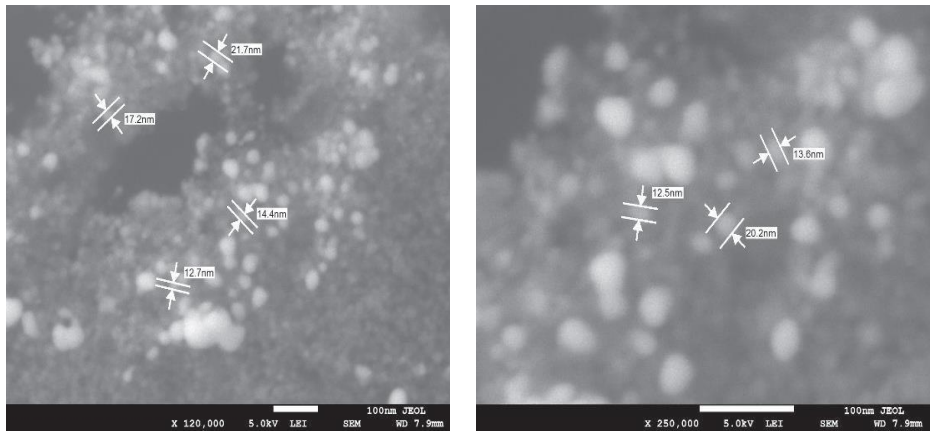

(a) (b)

Figure 14: FESEM image of AgNPs biosynthesized using *A. indica* leaf extract at magnification. (a) 120,000x and (b) 250,000x.

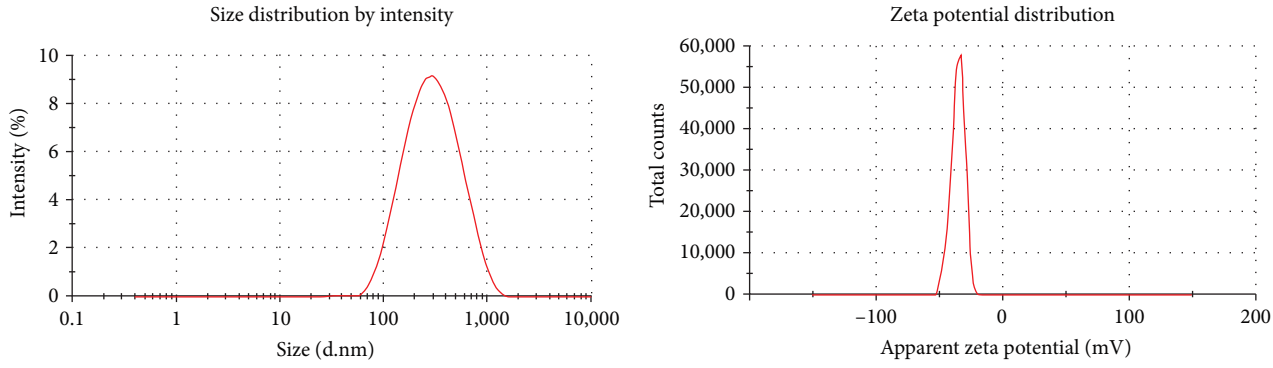

(a) (b)

Figure 15: (a) DLS and (b) zeta potential analysis of AgNPs biosynthesized using *A. indica* fruit extract.

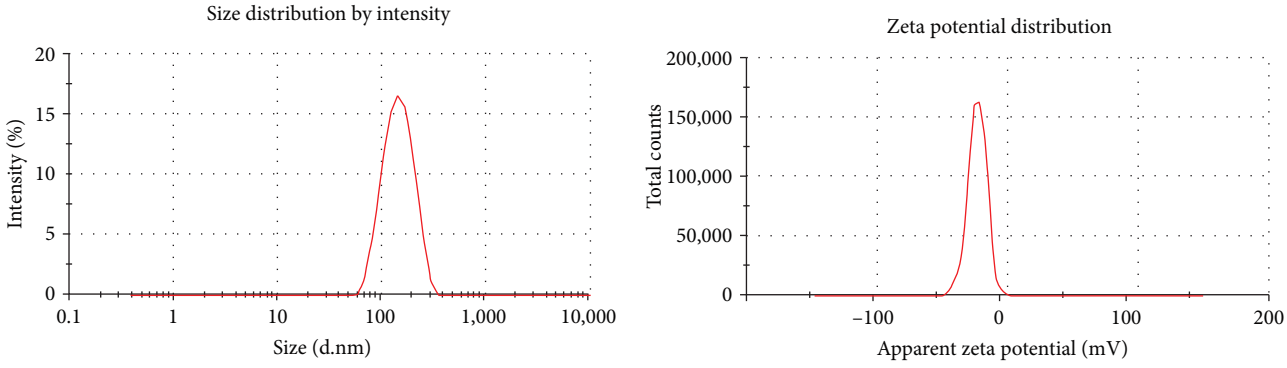

(a) (b)

Figure 16: (a) DLS and (b) zeta potential analysis of AgNPs biosynthesized using *A. indica* leaf extract.

had a polydispersity index (PDI) of 0.24 and 0.29, respectively, which is satisfactory for drug delivery applications [61]. PDI is an indicator of the stability and dispersity of nanoparticles; thus, nanoparticles with a PDI less than 0.5 are considered monodispersed and stable [62]. A previous study [63] reported similar particle sizes of AgNPs synthesized from *Rheum palmatum* root extracts.

The zeta potential evaluates the stability and surface charge of AgNPs. AgNPs synthesized from *A. indica* fruit extract exhibited a zeta potential of −35 mV (Figure 15(b)).

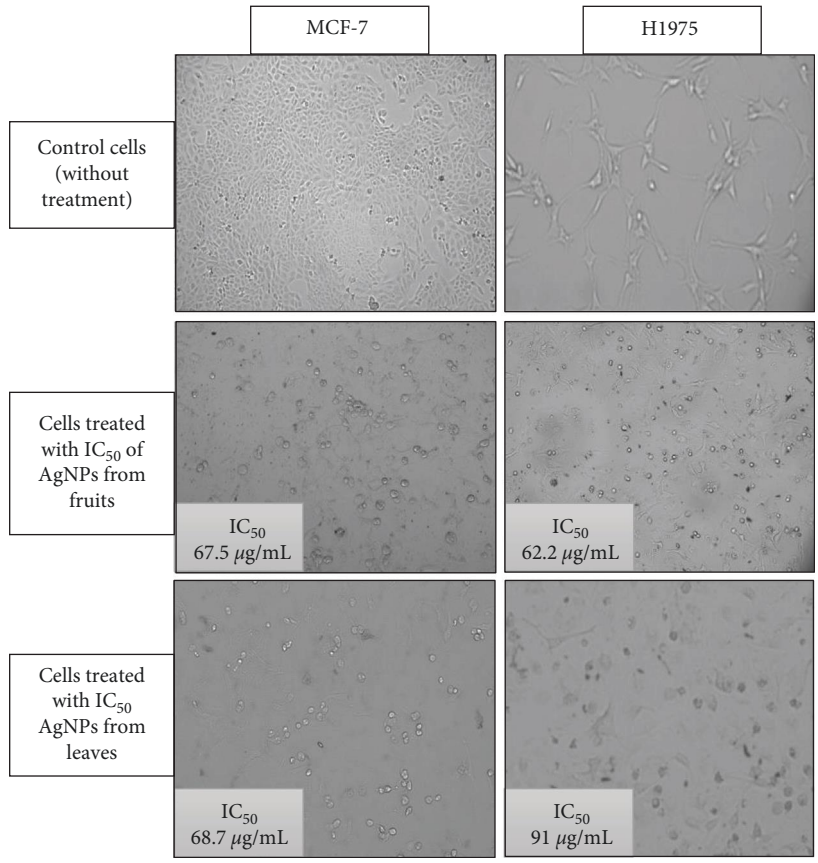

Figure 17: Inverted microscope images at a 10x magnification for MCF-7 and H1975 cancer cell lines before and after treating with AgNPs synthesized from the extracts of *A. indica* fruits and leaves.

By contrast, those synthesized from *A. indica* leaf extracts had a zeta potential of −23 mV (Figure 16(b)). An extract capped by nanoparticles has a negative zeta potential [64]. Generally, nanoparticles with zeta potentials ranging from −20 to −30 mV are moderately stable [65]. Hence, AgNPs synthesized from *A. indica* fruit were more stable than AgNPs synthesized from leaf extract. These findings are significant compared to previous findings [55]. This study suggests that *A. indica* fruit extract can produce stable AgNPs with precise morphologies and yields, supporting various applications, including antibacterial, antiviral, antifungal, anti-inflammatory, and anticancer activities.

3.3. Anticancer Properties of AgNPs. Recent studies have suggested that AgNPs may act as therapeutic agents for cancer treatment because of their unique properties [66]. This study was conducted to test the anticancer activity of AgNPs in breast (MCF-7) and lung (H1975) cancer cell lines. Figure 17 shows images of the cells obtained using an inverted microscope (Leitz, Wetzlar, Germany). As observed with an inverted microscope, treatment with AgNPs caused the MCF-7 and H1975 cells to lose their typical morphological characteristics, and many shrinkage and necrotic cells were detected following exposure to AgNPs compared to untreated control cells (Figure 17). The results demonstrated a decrease in cell viability for both cancer cell lines with increasing concentrations of AgNPs, suggesting the cytotoxicity of the nanoparticles against cancer cells (Figure 18). A previous study reported that AgNPs could be cytotoxic to breast and lung cancer cells, depending on their concentration [67]. AgNPs' anticancer properties are due to their induction of ROS in the cells, which stimulates apoptosis, autophagy, and necrosis [68]. The results of the MTT assay showed that AgNPs biosynthesized from *A. indica* fruit extract had more cytotoxic effects on H1975 lung cancer cells than AgNPs produced using *A. indica* leaf extract, with IC_{50} of 62.2 and 91 μg/mL, respectively. This difference in cytotoxicity may be attributed to the fact that fruit extract contains more phytochemicals than leaves. The apoptotic action of small nanoparticles appears to be mediated by their uptake into nuclei within the intracellular membrane, which varies from the uptake of larger particles. A previous study reported that nanoparticles with a size of 50 nm could be rapidly and efficiently incorporated by mammalian cells via endocytosis compared to other sizes [69]. However, cells had a much lower uptake of nanoparticles larger than 50 nm. The researchers also demonstrated that smaller AgNPs are more capable of causing apoptosis in MC3T3-E1 cells than larger AgNPs. Small AgNPs are more toxic because of their larger surface areas, which release silver ions faster,

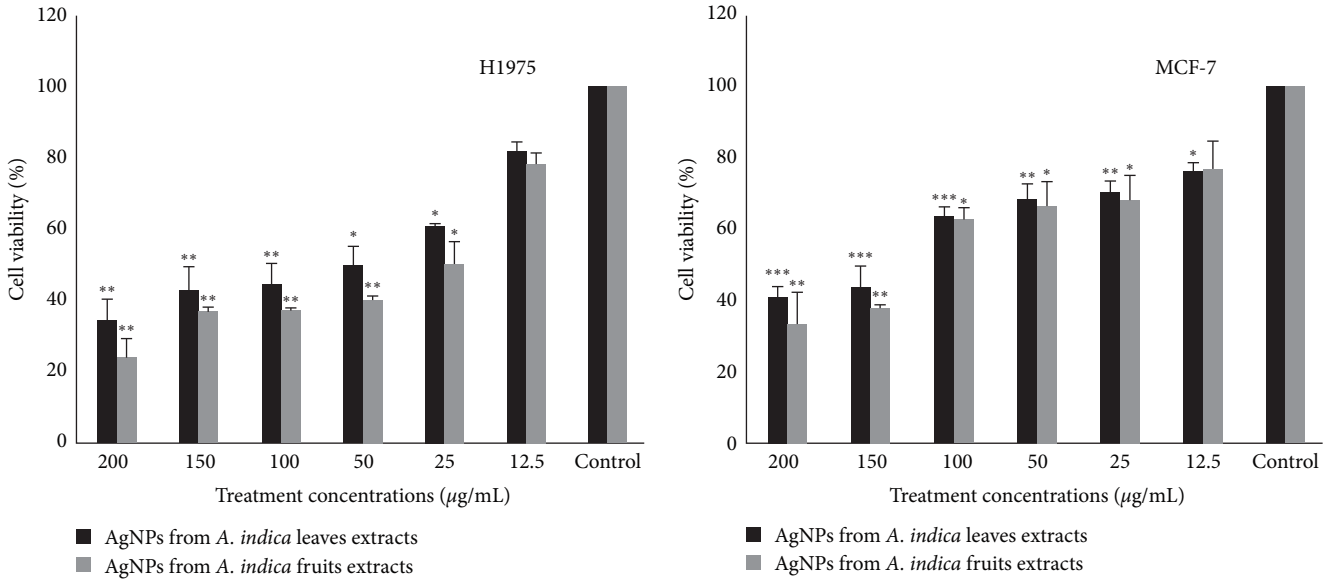

FIGURE 18: MTT assay analysis of the effect of green synthesized AgNPs using *A. indica* fruit and leaf extracts on H1975 and MCF-7 cell lines. Three independent experiments were performed to determine the mean and ± SD. The *P*-value ($^{***}P \leq 0.001$, $^{**}P \leq 0.01$, $^{*}P \leq 0.05$) was obtained by using one-way ANOVA and Tukey post hoc tests of variance with SPSS software version 28.0 (SPSS, Inc., Chicago, IL, USA).

activating ROS and resulting in apoptosis. The larger surface area of nanoparticles allows for better penetration and metal activity [28].

Besides the nanoparticles' size, the surface charge is considered one of the most critical factors governing AgNPs' toxicity [70]. The AgNPs cytotoxicity mechanism combines the effects of surface charge and a release of silver ions from nanoparticles. The surface charge of AgNPs is crucial for the development of responses of cells to stress action. It plays a significant role in binding proteins, changing the AgNPs' physical and chemical properties. As the surface charge increases, the toxicity of nanoparticles increases. AgNPs biosynthesized from fruits and leaves showed similar cytotoxic effects on MCF-7 cells, with IC_{50} values of 67.5 and 68.7 μg/mL, respectively. In this study, AgNPs from *A. indica* leaf extract show better toxicity against MCF-7 cells than previously reported [71]. Moreover, plant-derived AgNPs' toxicity levels may vary depending on the target cells, extraction solvents, collection site, and study period. Media ionize AgNPs differently, influencing their cytotoxicity on cancer cells. A previous study dissolved AgNPs in three diffusion media (PBS, deionized water, and cell culture medium), and silver ions were detected at high concentrations in deionized water [72]. A recent study investigated the stability of AgNPs by measuring absorbance at 100–900 nm in PBS buffer, distilled water, complete medium, DMEM, and NaCl (0.9%) over 28 days [73], and the results showed shelf stability of AgNPs in distilled water.

The cytotoxicity of AgNPs against cancer cells could be determined by activating lactate dehydrogenase and ROS, leading to the induction of apoptosis [29]. The apoptosis of cancer cells was confirmed in the host by the resulting nuclear fragmentation, in which the accumulation of ROS and oxidative stress causes physiological and cellular events,

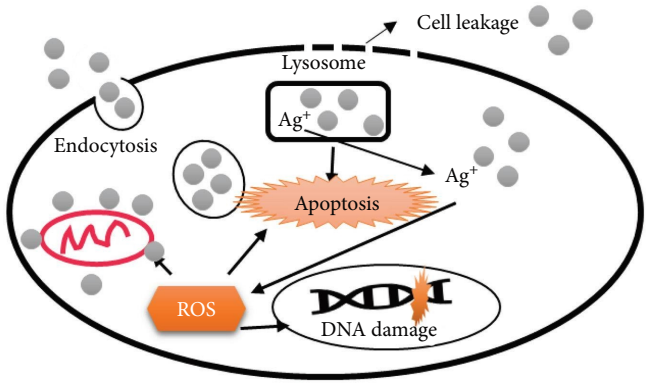

FIGURE 19: Mechanisms of anticancer activity of AgNPs.

including stress, mitochondrial disruption and destruction, apoptosis, inflammation, and DNA damage. ROS levels illustrate the induction of apoptosis and are involved in DNA damage. AgNPs were shown to efficiently induce cell death in HeLA cells by arresting their cell cycle at Sub G1 [53]. Figure 19 shows the mechanism of the anticancer activity of AgNPs. The ability of a treatment to selectively cause apoptosis in cancer cells while sparing healthy cells is an essential requirement for effective cancer treatment. In this regard, earlier investigations reported that AgNPs were less toxic to healthy cells than cancer cells, highlighting the potential application of AgNPs as an anticancer treatment. For instance, Singh et al. [74] demonstrated a deficient level of toxicity of the AgNPs produced from *papaya* leaf extract against normal HaCaT cells and Farahani et al. [75] also reported less toxicity of the AgNPs biosynthesized using *Amigdalus spinosissima* against normal L929 cells.

Table 1: Properties of AgNPs biosynthesized from *A. indica* based on recent studies.

A. indica part	Size (DLS)	Size (SEM)	Zeta potential	IC_{50} concentration of AgNPs against cancer cells	Reference
Leaves	38.5 nm	–	−33.2 mV	0.90 ± 0.07 mg/mL for MCF-7 cell lines	[71]
Leaves	–	20–50 nm	–	15.6 μg/mL against human acute lymphoblastic leukemia cells	[21]
Barks	58.8 nm	–	−33 mV	8.02 ± 0.18 μg/mL against human prostate cancer cells (DU-145)	[76]
Leaves	145.7 nm	44.04–66.50 nm	−55.3 mV	As AgNPs showed no IC_{50} value on V79 cells, they were considered low cytotoxic in the concentration ranges	[77]
Fruits	249 nm	27 nm	−35.6 mV	Against A549, bioAgNPs have an IC_{50} of 64.46 μg/mL	[25]

Table 2: Properties of AgNPs biosynthesized from *A. indica* based on this study.

A. indica part	Size (DLS)	Size (SEM)	Zeta potential	IC_{50} concentration of AgNPs against cancer cells
Leaves	160 nm	18.7 nm	−23 mV	AgNPs have an IC_{50} of 91 μg/mL against H1975, while AgNPs have an IC_{50} of 68.7 μg/mL against MCF-7
Fruits	245 nm	14.5 nm	−35 mV	The IC_{50} of AgNPs against H1975 is 62.2 μg/mL, and against MCF-7 it is 67.5 μg/mL

Tables 1 and 2 summarize several important properties of AgNPs biosynthesized from *A. indica* based on recent studies and this study. The tables highlight that this study was able to fabricate AgNPs with smaller sizes and higher toxicity against cancer cells than those reported in previous studies.

4. Conclusions

In recent years, there has been an extensive effort toward developing safer ways to synthesize AgNPs. Different characterization techniques were used to estimate the morphology of AgNPs, prepared from various medicinal plants, with varying shape and size distributions, which poses a severe challenge in their application. In this context, the plant extract volume, reaction temperature, silver salt concentration, reaction time, and pH value may play a vital role in achieving the desired shape and size of AgNPs. Hence, the AgNPs in this study were synthesized using the extracts of *A. indica* leaves and fruits. The synthesis was optimized to synthesis nanoparticles with the desired morphologies. In addition, AgNPs were characterized using UV−Vis spectroscopy, FTIR, FESEM, DLS, and zeta potential measurements. The cytotoxicity of green-synthesized AgNPs against lung and breast cancer cell lines was assessed using the MTT assay. The findings suggest that *A. indica* fruit and leaf extracts are suitable for synthesizing AgNPs with high yields and short production times. In addition, this study found that bioAgNPs are effective against lung and breast cancer; however, further research is needed to evaluate the effect of AgNPs on healthy cells.

Data Availability

The data used to support the findings of this study are included in the article.

Conflicts of Interest

The authors declare that there is no conflict of interest regarding the publication of this article.

Authors' Contributions

Nehad S. Alsubhi contributed to performing the literature search, experiments, and data analysis and preparing and writing the manuscript. Njud S. Alharbi had the idea for the article and contributed to supervising, critically editing, revising the manuscript, and approving its final version.

Acknowledgments

This research work was funded by Institutional Fund Projects under grant no. (IFPIP: 240-247-1443). The authors gratefully acknowledge the technical and financial support provided by the Ministry of Education and King Abdulaziz University, DSR, Jeddah, Saudi Arabia.

References

[1] T. Ali, M. F. Warsi, S. Zulfiqar et al., "Green nickel/nickel oxide nanoparticles for prospective antibacterial and environmental remediation applications," *Ceramics International*, vol. 48, no. 6, pp. 8331–8340, 2022.

[2] V. A. Spirescu, C. Chircov, A. M. Grumezescu, B. S. Vasile, and E. Andronescu, "Inorganic nanoparticles and composite films for antimicrobial therapies," *International Journal of Molecular Sciences*, vol. 22, no. 9, Article ID 4595, 2021.

[3] A. Desireddy, B. E. Conn, J. Guo et al., "Ultrastable silver nanoparticles," *Nature*, vol. 501, no. 7467, pp. 399–402, 2013.

[4] M. Kandiah and K. N. Chandrasekaran, "Green synthesis of silver nanoparticles using *Catharanthus roseus* flower extracts and the determination of their antioxidant, antimicrobial, and photocatalytic activity," *Journal of Nanotechnology*, vol. 2021, Article ID 5512786, 18 pages, 2021.

[5] N. S. Alharbi, N. S. Alsubhi, and A. I. Felimban, "Green synthesis of silver nanoparticles using medicinal plants: characterization and application," *Journal of Radiation Research and Applied Sciences*, vol. 15, no. 3, pp. 109–124, 2022.

[6] S. Kumari, P. K. Choudhary, R. Shukla, A. Sahebkar, and P. Kesharwani, "Recent advances in nanotechnology based combination drug therapy for skin cancer," *Journal of Biomaterials Science, Polymer Edition*, vol. 33, no. 11, pp. 1435–1468, 2022.

[7] T. Akshaya, M. Aravind, S. M. Kumar, and B. Divya, "Evaluation of in-vitro antibacterial activity against gram-negative bacteria using silver nanoparticles synthesized from *Dypsis lutescens* leaf extract," *Journal of the Chilean Chemical Society*, vol. 67, no. 2, pp. 5477–5483, 2022.

[8] S. Some, O. Bulut, K. Biswas et al., "Effect of feed supplementation with biosynthesized silver nanoparticles using leaf extract of *Morus indica* L. V1 on *Bombyx mori* L. (Lepidoptera: Bombycidae)," *Scientific Reports*, vol. 9, no. 1, pp. 1–13, 2019.

[9] M. S. Samuel, M. Ravikumar, J. A. John et al., "A review on green synthesis of nanoparticles and their diverse biomedical and environmental applications," *Catalysts*, vol. 12, no. 5, Article ID 459, 2022.

[10] I. Karmous, A. Pandey, K. B. Haj, and A. Chaoui, "Efficiency of the green synthesized nanoparticles as new tools in cancer therapy: insights on plant-based bioengineered nanoparticles, biophysical properties, and anticancer roles," *Biological Trace Element Research*, vol. 196, no. 1, pp. 330–342, 2020.

[11] S. V. Ganachari, J. S. Yaradoddi, S. B. Somappa et al., "Green nanotechnology for biomedical, food, and agricultural applications," *Handbook of Ecomaterials*, vol. 4, pp. 2681–2689, 2019.

[12] L. V. Hublikar, S. V. Ganachari, N. Raghavendra, V. B. Patil, and N. R. Banapurmath, "Green synthesis silver nanoparticles via *Eichhornia crassipes* leaves extract and their applications," *Current Research in Green and Sustainable Chemistry*, vol. 4, Article ID 100212, 2021.

[13] L. V. Hublikar, S. V. Ganachari, N. Raghavendra et al., "Biogenesis of silver nanoparticles and its multifunctional anti-corrosion and anticancer studies," *Coatings*, vol. 11, no. 10, Article ID 1215, 2021.

[14] E. I. Murillo-Rábago, A. R. Vilchis-Nestor, K. Juarez-Moreno, L. E. Garcia-Marin, K. Quester, and E. Castro-Longoria, "Optimized synthesis of small and stable silver nanoparticles using intracellular and extracellular components of fungi: an alternative for bacterial inhibition," *Antibiotics*, vol. 11, no. 6, Article ID 800, 2022.

[15] A. Bergal, G. H. Matar, and M. Andaç, "Olive and green tea leaf extracts mediated green synthesis of silver nanoparticles (AgNPs): comparison investigation on characterizations and antibacterial activity," *BioNanoScience*, vol. 12, no. 2, pp. 307–321, 2022.

[16] K. Chand, D. Cao, D. E. Fouad et al., "Green synthesis, characterization and photocatalytic application of silver nanoparticles synthesized by various plant extracts," *Arabian Journal of Chemistry*, vol. 13, no. 11, pp. 8248–8261, 2020.

[17] V. Sharma, S. Kaushik, P. Pandit, D. Dhull, J. P. Yadav, and S. Kaushik, "Green synthesis of silver nanoparticles from medicinal plants and evaluation of their antiviral potential against chikungunya virus," *Applied Microbiology and Biotechnology*, vol. 103, no. 2, pp. 881–891, 2019.

[18] S. Some, I. K. Sen, A. Mandal et al., "Biosynthesis of silver nanoparticles and their versatile antimicrobial properties," *Materials Research Express*, vol. 6, no. 1, Article ID 012001, 2018.

[19] S. Na'ala and S. Sufiyanu, "Antimicrobial activity of neem (*Azadirachta indica* A. Juss.) aqueous and methanolic extracts against pathogenic bacteria (*Staphylococcus aureus*) and fungi (*Candida albicans*)," *International Journal of Science for Global Sustainability*, vol. 8, no. 1, Article ID 5, 2022.

[20] M. Damtew, "A review on chemical composition, medicinal value and other applications of *Azadirachta indica*," *Agricultural and Biological Research*, vol. 38, no. 2, pp. 268–272, 2022.

[21] M. Asimuddin, M. R. Shaik, S. F. Adil et al., "*Azadirachta indica* based biosynthesis of silver nanoparticles and evaluation of their antibacterial and cytotoxic effects," *Journal of King Saud University—Science*, vol. 32, no. 1, pp. 648–656, 2020.

[22] P. Roy, B. Das, A. Mohanty, and S. Mohapatra, "Green synthesis of silver nanoparticles using *Azadirachta indica* leaf extract and its antimicrobial study," *Applied Nanoscience*, vol. 7, no. 8, pp. 843–850, 2017.

[23] H. Tateishi-Karimata and N. Sugimoto, "Roles of non-canonical structures of nucleic acids in cancer and neurodegenerative diseases," *Nucleic Acids Research*, vol. 49, no. 14, pp. 7839–7855, 2021.

[24] B. D. Altinsoy, G. Ş. Karatoprak, and I. Ocsoy, "Extracellular directed ag NPs formation and investigation of their antimicrobial and cytotoxic properties," *Saudi Pharmaceutical Journal*, vol. 27, no. 1, pp. 9–16, 2019.

[25] N. S. Alharbi and N. S. Alsubhi, "Green synthesis and anticancer activity of silver nanoparticles prepared using fruit extract of *Azadirachta indica*," *Journal of Radiation Research and Applied Sciences*, vol. 15, no. 3, pp. 335–345, 2022.

[26] E. M. Halawani, "Rapid biosynthesis method and characterization of silver nanoparticles using *Zizyphus spina christi* leaf extract and their antibacterial efficacy in therapeutic application," *Journal of Biomaterials and Nanobiotechnology*, vol. 8, no. 1, pp. 22–35, 2016.

[27] C. H. Lee, T. H. Lee, P. Y. Ong et al., "Integrated ultrasound-mechanical stirrer technique for extraction of total alkaloid content from *Annona muricata*," *Process Biochemistry*, vol. 109, pp. 104–116, 2021.

[28] A. Nzekekwu and O. Abosede, "Green synthesis and characterization of silver nanoparticles using leaves extracts of neem (*Azadirachta indica*) and bitter leaf (*Vernonia amygdalina*)," *Journal of Applied Sciences and Environmental Management*, vol. 23, no. 4, pp. 695–699, 2019.

[29] S. Ahmed, M. Ahmad, B. L. Swami, and S. Ikram, "Green synthesis of silver nanoparticles using *Azadirachta indica* aqueous leaf extract," *Journal of Radiation Research and Applied Sciences*, vol. 9, no. 1, pp. 1–7, 2016.

[30] O. Stavinskaya, I. Laguta, T. Fesenko, and M. Krumova, "Effect of temperature on green synthesis of silver nanoparticles using

Vitex agnus-castus extract," *Chemistry Journal of Moldova*, vol. 14, no. 2, pp. 117–121, 2019.

[31] H. M. Kredy, "The effect of pH, temperature on the green synthesis and biochemical activities of silver nanoparticles from *Lawsonia inermis* extract," *Journal of Pharmaceutical Sciences and Research*, vol. 10, no. 8, pp. 2022–2026, 2018.

[32] S. K. Srikar, D. D. Giri, D. B. Pal, P. K. Mishra, and S. N. Upadhyay, "Light induced green synthesis of silver nanoparticles using aqueous extract of *Prunus amygdalus*," *Green and Sustainable Chemistry*, vol. 6, no. 1, pp. 26–33, 2016.

[33] B. M. H. Ali, "Eco-friendly synthesis of silver nanoparticles from crust of Cucurbita Maxima L.(red pumpkin)," *EurAsian Journal of BioSciences*, vol. 14, no. 2, pp. 2829–2833, 2020.

[34] J. Osorio-Echavarría, J. Osorio-Echavarría, C. P. Ossa-Orozco, and N. A. Gómez-Vanegas, "Synthesis of silver nanoparticles using white-rot fungus Anamorphous *Bjerkandera* sp. R1: influence of silver nitrate concentration and fungus growth time," *Scientific Reports*, vol. 11, no. 1, pp. 1–14, 2021.

[35] T. Adak, H. Swain, S. Munda et al., "Green silver nanoparticles: synthesis using rice leaf extract, characterization, efficacy, and non-target effects," *Environmental Science and Pollution Research*, vol. 28, no. 4, pp. 4452–4462, 2021.

[36] M. M. I. Masum, M. M. Siddiqa, K. A. Ali et al., "Biogenic synthesis of silver nanoparticles using *Phyllanthus emblica* fruit extract and its inhibitory action against the pathogen *Acidovorax oryzae* strain RS-2 of rice bacterial brown stripe," *Frontiers in Microbiology*, vol. 10, Article ID 820, 2019.

[37] S. Satpathy, A. Patra, B. Ahirwar, and M. Delwar Hussain, "Antioxidant and anticancer activities of green synthesized silver nanoparticles using aqueous extract of tubers of *Pueraria tuberosa*," *Artificial Cells, Nanomedicine, and Biotechnology*, vol. 46, no. Suppl. 3, pp. S71–S85, 2018.

[38] R. Vijayabharathi, A. Sathya, and S. Gopalakrishnan, "Extracellular biosynthesis of silver nanoparticles using *Streptomyces griseoplanus* SAI-25 and its antifungal activity against *Macrophomina phaseolina*, the charcoal rot pathogen of sorghum," *Biocatalysis and Agricultural Biotechnology*, vol. 14, pp. 166–171, 2018.

[39] A. Moshfegh, A. Jalali, A. Salehzadeh, and A. Sadeghi Jozani, "Biological synthesis of silver nanoparticles by cell-free extract of *Polysiphonia algae* and their anticancer activity against breast cancer MCF-7 cell lines," *Micro & Nano Letters*, vol. 14, no. 5, pp. 581–584, 2019.

[40] J. S. Moodley, S. B. N. Krishna, K. Pillay, F. Sershen, and P. Govender, "Green synthesis of silver nanoparticles from *Moringa oleifera* leaf extracts and its antimicrobial potential," *Advances in Natural Sciences: Nanoscience and Nanotechnology*, vol. 9, no. 1, Article ID 015011, 2018.

[41] A. Afreen, R. Ahmed, S. Mehboob et al., "Phytochemical-assisted biosynthesis of silver nanoparticles from *Ajuga bracteosa* for biomedical applications," *Materials Research Express*, vol. 7, no. 7, Article ID 075404, 2020.

[42] S. G. Eswaran, M. A. Ashkar, M. H. Mamat et al., "Preparation of a portable calorimetry kit and one-step spectrophotometric nanomolar level detection of L-Histidine in serum and urine samples using sebacic acid capped silver nanoparticles," *Journal of Science: Advanced Materials and Devices*, vol. 6, no. 1, pp. 100–107, 2021.

[43] M. Maruthupandi, M. Chandhru, S. K. Rani, and N. Vasimalai, "Highly selective detection of iodide in biological, food, and environmental samples using polymer-capped silver nanoparticles: preparation of a paper-based testing kit for on-site monitoring," *ACS Omega*, vol. 4, no. 7, pp. 11372–11379, 2019.

[44] G. Sharma, J.-S. Nam, A. R. Sharma, and S. S. Lee, "Antimicrobial potential of silver nanoparticles synthesized using medicinal herb *Coptidis rhizome*," *Molecules*, vol. 23, no. 9, Article ID 2268, 2018.

[45] C. Tyavambiza, A. M. Elbagory, A. M. Madiehe, M. Meyer, and S. Meyer, "The antimicrobial and anti-inflammatory effects of silver nanoparticles synthesised from *Cotyledon orbiculata* aqueous extract," *Nanomaterials*, vol. 11, no. 5, Article ID 1343, 2021.

[46] A. Verma and M. S. Mehata, "Controllable synthesis of silver nanoparticles using Neem leaves and their antimicrobial activity," *Journal of Radiation Research and Applied Sciences*, vol. 9, no. 1, pp. 109–115, 2016.

[47] P. K. J. D. M. Upadhaya and M. K. Tiwari, "Synthesis of silver nano particles by *Azadirachta indica* aqueous leaf extract and characterization of silver nanoparticles, used for pharmaceutical," *Journal of Natural Remedies*, vol. 1, no. 1, pp. 326–334, 2021.

[48] M. Mankad, G. Patil, D. Patel, P. Patel, and A. Patel, "Comparative studies of sunlight mediated green synthesis of silver nanoparticles from *Azadirachta indica* leaf extract and its antibacterial effect on *Xanthomonas oryzae* pv. *oryzae*," *Arabian Journal of Chemistry*, vol. 13, no. 1, pp. 2865–2872, 2020.

[49] V. T. Nguyen, "Sunlight-driven synthesis of silver nanoparticles using pomelo peel extract and antibacterial testing," *Journal of Chemistry*, vol. 2020, Article ID 6407081, 9 pages, 2020.

[50] F. Y. Alzoubi, J. Y. Al-zou'by, S. K. Theban, M. K. Alqadi, H. M. Al-khateeb, and E. S. AlSharo, "Size, stability, and aggregation of citrates-coated silver nanoparticles: contribution of background electrolytes," *Nanotechnology for Environmental Engineering*, vol. 6, no. 3, pp. 1–7, 2021.

[51] R. R. Nasaruddin, S. Engliman, and M. S. Mastuli, "Green synthesis of silver nanoparticles using coffee extract for catalysis," *Malaysian NANO-An International Journal*, vol. 1, no. 2, pp. 13–25, 2021.

[52] A. Sidorowicz, T. Szymański, and J. D. Rybka, "Photodegradation of biohazardous dye brilliant blue R using organometallic silver nanoparticles synthesized through a green chemistry method," *Biology*, vol. 10, no. 8, Article ID 784, 2021.

[53] M. S. Jabir, A. A. Hussien, G. M. Sulaiman et al., "Green synthesis of silver nanoparticles from *Eriobotrya japonica* extract: a promising approach against cancer cells proliferation, inflammation, allergic disorders and phagocytosis induction," *Artificial Cells, Nanomedicine, and Biotechnology*, vol. 49, no. 1, pp. 48–60, 2021.

[54] P. Senthilkumar, S. Rashmitha, P. Veera, C. V. Ignatious, C. SaiPriya, and A. V. Samrot, "Antibacterial activity of neem extract and its green synthesized silver nanoparticles against *Pseudomonas aeruginosa*," *Journal of Pure and Applied Microbiology*, vol. 12, no. 2, pp. 969–974, 2018.

[55] K. Ramar and A. J. Ahamed, "Hydrothermal green synthesis of silver nanoparticles using *Azadirachta indica* A. Juss. fruit juice for potential antibacterial activity," *Journal of Nanoscience and Technology*, vol. l, pp. 519–523, 2018.

[56] C. G. Mariana, H. G. Carlos, M. Jaqueline, M. B. Taís, and V. S. Luís, "Phytochemical screening of *Azadirachta indica* A. Juss for antimicrobial activity," *African Journal of Microbiology Research*, vol. 11, no. 4, pp. 117–122, 2017.

[57] M. Ziąbka, E. Menaszek, J. Tarasiuk, and S. Wroński, "Biocompatible nanocomposite implant with silver nanoparticles for otology—in vivo evaluation," *Nanomaterials*, vol. 8, no. 10, Article ID 764, 2018.

[58] N. P. Truong, M. R. Whittaker, C. W. Mak, and T. P. Davis, "The importance of nanoparticle shape in cancer drug delivery," *Expert Opinion on Drug Delivery*, vol. 12, no. 1, pp. 129–142, 2015.

[59] H. Chugh, D. Sood, I. Chandra, V. Tomar, G. Dhawan, and R. Chandra, "Role of gold and silver nanoparticles in cancer nano-medicine," *Artificial Cells, Nanomedicine, and Biotechnology*, vol. 46, no. Suppl. 1, pp. 1210–1220, 2018.

[60] K. Kartini, A. Alviani, D. Anjarwati, A. F. Fanany, J. Sukweenadhi, and C. Avanti, "Process optimization for green synthesis of silver nanoparticles using Indonesian medicinal plant extracts," *Processes*, vol. 8, no. 8, Article ID 998, 2020.

[61] M. Danaei, M. Dehghankhold, S. Ataei et al., "Impact of particle size and polydispersity index on the clinical applications of lipidic nanocarrier systems," *Pharmaceutics*, vol. 10, no. 2, Article ID 57, 2018.

[62] A. O. Fadaka, S. Meyer, O. Ahmed et al., "Broad spectrum antibacterial activity and non-selective toxicity of gum arabic silver nanoparticles," *International Journal of Molecular Sciences*, vol. 23, no. 3, Article ID 1799, 2022.

[63] S. Arokiyaraj, S. Vincent, M. Saravanan, Y. Lee, Y. K. Oh, and K. H. Kim, "Green synthesis of silver nanoparticles using *Rheum palmatum* root extract and their antibacterial activity against *Staphylococcus aureus* and *Pseudomonas aeruginosa*," *Artificial Cells, Nanomedicine, and Biotechnology*, vol. 45, no. 2, pp. 372–379, 2017.

[64] M. Reda, A. Ashames, Z. Edis, S. Bloukh, R. Bhandare, and H. Abu Sara, "Green synthesis of potent antimicrobial silver nanoparticles using different plant extracts and their mixtures," *Processes*, vol. 7, no. 8, Article ID 510, 2019.

[65] H. Singh, J. Du, P. Singh, and T. H. Yi, "Role of green silver nanoparticles synthesized from *Symphytum officinale* leaf extract in protection against UVB-induced photoaging," *Journal of Nanostructure in Chemistry*, vol. 8, no. 3, pp. 359–368, 2018.

[66] S. Bhatnagar, T. Kobori, D. Ganesh, K. Ogawa, and H. Aoyagi, "Biosynthesis of silver nanoparticles mediated by extracellular pigment from *Talaromyces purpurogenus* and their biomedical applications," *Nanomaterials*, vol. 9, no. 7, Article ID 1042, 2019.

[67] Ş. Yeşilot and S. Dönmez, "Cytotoxic effect of green synthesized silver nanoparticles with *Salvia officinalis* on MCF-7 human breast cancer cells," *Turkish Journal of Health Science and Life*, vol. 4, no. 3, pp. 133–139, 2021.

[68] A. Andleeb, A. Andleeb, S. Asghar et al., "A systematic review of biosynthesized metallic nanoparticles as a promising anti-cancer-strategy," *Cancers*, vol. 13, no. 11, Article ID 2818, 2021.

[69] T.-H. Kim, M. Kim, H.-S. Park, U. S. Shin, M.-S. Gong, and H.-W. Kim, "Size-dependent cellular toxicity of silver nanoparticles," *Journal of Biomedical Materials Research Part A*, vol. 100, no. 4, pp. 1033–1043, 2012.

[70] E. Matras, A. Gorczyca, E. Pociecha, S. W. Przemieniecki, and M. Oćwieja, "Phytotoxicity of silver nanoparticles with different surface properties on monocots and dicots model plants," *Journal of Soil Science and Plant Nutrition*, vol. 22, pp. 1647–1664, 2022.

[71] S. A. Kumari, A. K. Patlolla, and P. Madhusudhanachary, "Biosynthesis of silver nanoparticles using *Azadirachta indica* and their antioxidant and anticancer effects in cell lines," *Micromachines*, vol. 13, no. 9, Article ID 1416, 2022.

[72] M. Wypij, T. Jędrzejewski, J. Trzcińska-Wencel, M. Ostrowski, M. Rai, and P. Golińska, "Green synthesized silver nanoparticles: antibacterial and anticancer activities, biocompatibility, and analyses of surface-attached proteins," *Frontiers in Microbiology*, vol. 12, Article ID 632505, 2021.

[73] Y. Xue, T. Zhang, B. Zhang, F. Gong, Y. Huang, and M. Tang, "Cytotoxicity and apoptosis induced by silver nanoparticles in human liver HepG2 cells in different dispersion media," *Journal of Applied Toxicology*, vol. 36, no. 3, pp. 352–360, 2016.

[74] S. P. Singh, A. Mishra, R. K. Shyanti, R. P. Singh, and A. Acharya, "Silver nanoparticles synthesized using *Carica papaya* leaf extract (AgNPs-PLE) causes cell cycle arrest and apoptosis in human prostate (DU145) cancer cells," *Biological Trace Element Research*, vol. 199, no. 4, pp. 1316–1331, 2021.

[75] A. F. Farahani, S. M. M. Hamdi, and A. Mirzaee, "GC/MS analysis and phyto-synthesis of silver nanoparticles using *Amygdalus spinosissima* extract: antibacterial, antioxidant effects, anticancer and apoptotic effects," *Avicenna Journal of Medical Biotechnology*, vol. 14, pp. 223–232, 2022.

[76] S. R. Kitimu, P. Kirira, J. Sokei, D. Ochwangi, P. Mwitari, and N. Maina, "Biogenic synthesis of silver nanoparticles using *Azadirachta indica* methanolic bark extract and their anti-proliferative activities against DU-145 human prostate cancer cells," *African Journal of Biotechnology*, vol. 21, no. 2, pp. 64–72, 2022.

[77] Y. Dutt, R. P. Pandey, M. Dutt et al., "Synthesis and biological characterization of phyto-fabricated silver nanoparticles from *Azadirachta indica*," *Journal of Biomedical Nanotechnology*, vol. 18, pp. 2022–2057, 2022.